Earthquakes and Structures, Vol. 2, No. 2 (2011) 109-126
DOI: http://dx.doi.org/10.12989/eas.2011.2.2.109

An assessment of code designed, torsionally stiff, asymmetric steel buildings under strong earthquake excitations

M.T. Kyrkos and S.A. Anagnostopoulos*

Department of Civil Engineering, University of Patras, 26500 Patras, Greece

(Received June 7, 2010, Accepted February 8, 2011)

Abstract. The inelastic earthquake response of non-symmetric, braced steel buildings, designed according to the EC3 (steel structures) and EC8 (earthquake resistant design) codes, is investigated using 1, 3 and 5-story models, subjected to a set of 10, two-component, semi-artificial motions, generated to match the design spectrum. It is found that in these buildings, the so-called "flexible" edge frames exhibit higher ductility demands and interstory drifts than the "stiff" edge frames. We note that the same results were reported in an earlier study for reinforced concrete buildings and are the opposite of what was predicted in several other studies based on the over simplified, hence very popular, one-story, shear-beam type models. The substantial differences in such demands between the two sides suggest a need for reassessment of the pertinent code provisions. In a follow up paper, a design modification will be introduced that can lead to a more uniform distribution of ductility demands in the elements of all building edges. This investigation is another step towards more rational design of non-symmetric steel buildings.

Keywords: asymmetry; eccentricity; torsion; multistory steel buildings; braces; earthquake inelastic response; plastic hinge model.

1. Introduction

Inelastic response of non symmetric buildings to strong earthquake motions is a very active area of research. Such response involves torsional motion that can be caused not only from the mass and stiffness eccentricities that are known when the building is designed, but also due to factors unknown at design time and hence difficult to account for directly. Such factors can be eccentric arrangements of "non-structural", yet load-bearing elements, non coherent input at support points or asymmetric yielding. Because some of these factors cannot be known in advance and hence be explicitly accounted for in design, torsion can make the response of the building more severe and thus increase damage or even contribute to collapse. Moreover, the fact that modern building code design addresses inelastic response in a highly approximate manner (based on elastic analyses with reduced seismic actions and through capacity design procedures), even the known eccentricities of buildings with irregular layouts can generate unexpected inelastic action.

Recent work has indicated that code designed, eccentric reinforced concrete frame buildings subjected to design level earthquake actions, exhibit undesirable inelastic response (Stathopoulos

* Corresponding author, Professor, E-mail: saa@upatras.gr

2001, Stathopoulos and Anagnostopoulos 2002, 2005). Using the response of the associated symmetric building as the basis for comparison, it has been found that frames at the "flexible" edges experience increased inelastic deformations and those at the "stiff" edges decreased deformations. As a result, inelastic response measures, such as ductility factors and damage indices, at the "flexible" edge have reached values more than twice those at the "stiff" edge. Obviously, such uneven distributions are undesirable as they can lead to premature member failures. We note here that this result is the opposite of what has been reported in past publications, based on simplified, highly idealized, one-story models, with simple shear-beam elements designed for lateral load resistance (Chandler and Duan 1991, Chopra and Goel 1991, Tso and Zhu 1992, Duan and Chandler 1993, Humar and Kumar 1999, Rutenberg 2002). Recently, however, it was shown that even the simplified, one story models predict the correct response, in qualitative agreement with the more detailed plastic hinge multistory models, provided that their element strengths are not determined only from the earthquake action but reflect the strengths of the realistic models determined for several loading conditions, including gravity loads (Anagnostopoulos *et al*. 2010).

In the present paper the distribution of earthquake induced ductility demands is examined for multistory, steel, eccentric buildings that are designed in accordance with the Eurocodes 3 (for steel) and 8 (for earthquake resistance). Three sets of buildings are designed: The first with one story, the second with 3 stories and the third with 5 stories. Each set includes a torsionally balanced building for reference and two eccentric buildings with mass eccentricities 0.10 and 0.20. A torsionally balanced building, defined as one that experiences no torsion under earthquake excitations, is designed so that its approximate stiffness center in each floor (defined below), coincides with the corresponding mass center. We note here that it would be easier to design and use totally symmetric buildings for reference in each of the three building groups, but these would have a slightly different layout from the eccentric buildings. It was therefore decided that a torsionally balanced building with the exact member layout as the eccentric buildings would be a more appropriate basis for comparisons. These buildings are subsequently subjected to sets of ten, two component semi-synthetic motions, generated to closely match the design response spectrum, and their rotational ductility demands as well as interstory drifts of the frames at the building edges are used to evaluate the building performance. An overloading with 1.5 times the design earthquake is also examined. Preliminary results of the work presented herein have been reported by Kyrkos and Anagnostopoulos (2010), but those were for buildings with symmetrically placed braces in the central bay of each of the four sides in the perimeter.

The objective of the work is to see if the behavior of the eccentric steel buildings is similar to the behavior reported earlier for reinforced concrete, eccentric, space frame buildings and if this happens it will point to an inherent problem with the applicable codes that will call for their modification.

2. Buildings and motions used

In the present study three sets of steel, braced frame buildings were selected: with one, three and five stories each. The layout is the same for all floors of all three buildings and may be seen in Fig. 1. In the same figure the elevations of the two sides of the 5 story building are also shown. Each building is formed by 4 frames along the x axis, (FR-1X to FR-4X) and 6 frames along the y axis (FR-1Y to FR-6Y). The exterior frames along the y axis have braces in the middle bay, while the

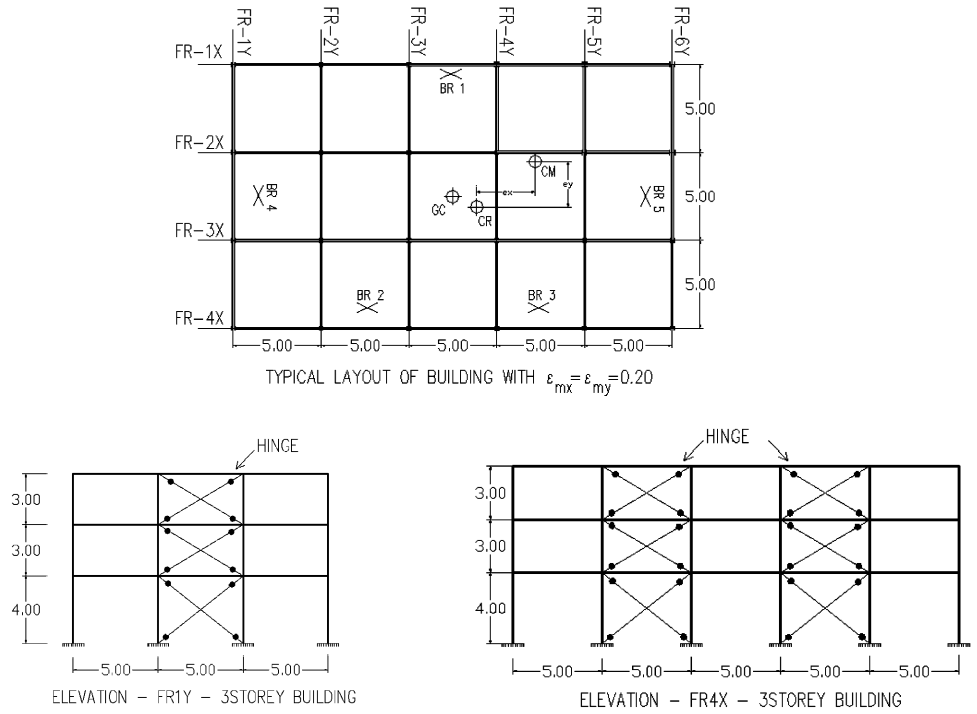

Fig. 1 Layout of 1, 3 and 5-storey buildings and x, y elevations of the 3-storey buildings

exterior frames along the x axes were selected each with a different number of braced bays: Frame - 1X has braces in its middle bay, while Frame - 4X at the opposite edge has braces in two bays, the second and fourth, symmetric about the middle. This difference in the braced bays of the two end frames along the x axis was a way to introduce an initial stiffness eccentricity. All buildings have a typical story height of 3.00 m and ground story height 4.00 m.

Using appropriate distributions of the floor loads, e.g. through non-symmetric live load distribution, non-symmetric balconies (common causes of mass eccentricity in typical Greek buildings, not shown in the given layout), non-symmetric joint masses were assigned at each floor and thus biaxial mass eccentricities were introduced in all floors. In this manner, in addition to the torsionally balanced layouts for each of the 1, 3 and 5-story buildings, eccentric variants were generated and designed with the following mass eccentricities: e_m = 0.10 L and e_m = 0.20 L, where L = building length along each direction. The models used for both design and analyses were 3-D models with masses lumped at the joints.

All buildings were designed as spatial frames for gravity and earthquake loads using the dynamic, response spectrum method, according to Eurocodes EC3- steel structures- and EC8-earthquake resistant design. For simplicity, all frame joints were assumed rigid. Earthquake actions were described by the design spectrum specified by the Greek Code for ground acceleration PGA = 0.24 g and soil category II. This spectrum can be seen in Fig. 2, along with the mean spectra of the motions used for subsequent analyses.

The dimensioning of the frame members took into account the uneven distribution of member forces due to the mass eccentricities and hence stiffness eccentricities were also generated, as it happens in actual practice. We note here that the building designs were carried out following the

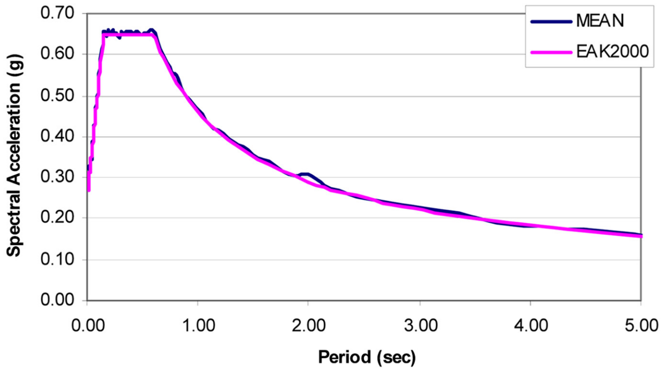

Fig. 2 Design spectrum for Greece and mean response spectrum of 10 semi artificial motions

Table 1 Eccentricities and fundamental periods of the buildings

Story number	Mass eccentricity	Mean natural eccentricity		Fundamental periods of buildings (sec)		
	$\varepsilon_{mx} = \varepsilon_{my}$	ε_x	ε_y	*Ty*	*Tx*	*Tθ*
1	0.00	0.00	0.00	0.340	0.290	0.195
	0.10	0.085	0.10	0.350	0.290	0.190
	0.20	0.15	0.18	0.355	0.295	0.180
3	0.00	0.00	0.00	0.570	0.495	0.330
	0.10	0.090	0.10	0.570	0.490	0.320
	0.20	0.140	0.185	0.570	0.495	0.310
5	0.00	0.00	0.00	0.920	0.800	0.540
	0.10	0.07	0.10	0.950	0.810	0.540
	0.20	0.14	0.185	0.900	0.820	0.510

two codes, EC3 and EC8, strictly and care was taken to use the minimum member sections that would satisfy ALL code provisions, so that no member would be overdesigned. Overdesigned members would mask the results and one could not obtain reliable conclusions.

The lowest, fundamental, periods of the symmetric building in each set are: $T_y = 0.345$ s (1-story), $T_y = 0.57$ s (3-story) and $T_y = 0.92$ s (5-story). The complete set of the lowest three periods of all building variants in each set is listed in Table 1, along with the initial mass eccentricities $\varepsilon_{mx} = \varepsilon_{my}$ (0.10 and 0.20) and the resulting physical eccentricities ε_x and ε_y. The latter are the mean distances (for all stories) between the mass center (CM) in each floor and the approximate stiffness center (CR) in the story, normalized by the length of the corresponding building side.

It is noted that in multistory buildings, the so called stiffness or rigidity center (CR) cannot be really defined, except under very restrictive conditions. Thus, an approximate CR was computed herein for reference purposes, on a floor by floor basis as follows (Eqs. (1) and (2))

$$e_{sx} = \frac{\sum_{i=1}^{m} K_{f-iy}\, x_i}{\sum_{1}^{m} K_{f-iy}} \qquad e_{sy} = \frac{\sum_{i=1}^{n} K_{f-ix}\, y_i}{\sum_{1}^{n} K_{f-ix}} \tag{1}$$

$$K_{f-i} = \frac{24E}{h^2}\left[\frac{2}{\sum K_c} + \frac{1}{\sum K_{ba}} + \frac{1}{\sum K_{bb}}\right]^{-1} + \sum \frac{AE}{L}\cos^2\varphi \tag{2}$$

where: e_{sx}, e_{sy} are the x and y coordinates of the approximate center of rigidity CR, $K_{f\text{-}i}$ designates the approximate story stiffness of frame i, x and y the directions of the frame axis, m and n the number of frames along the y and x axes, respectively, E = modulus of elasticity, $K_c = I_c/h$, $K_b = I_b/l$, I_c, I_b = section moment of inertia of columns and beams, respectively, h = story height and l = beam length, A = area of brace section, L = brace length and φ = angle of brace member and the horizontal plane. The second indices, a and b, in K_{ba} $\kappa\alpha\iota$ K_{bb} designate the upper (above) and lower (below) floor beams of the frame in the considered story. From Table 1 we can see that these physical eccentricities vary from 0.07 to 0.185. It is also noted that for all models, the first torsional period is lower than the two translational periods, so all buildings are torsionally stiff.

Each of the examined buildings, modeled as a non linear 3-D frame, was subjected to ten sets of two component semi-artificial motion pairs of biaxial motions. These motions were generated from a group of five, two-component, real earthquake records, to closely match the code design spectrum (with a descending branch $\propto 1/T^{2/3}$), using a method based on trial and error and Fourier transform techniques (Karabalis *et al*. 1994). As Fig. 2 indicates, the mean response spectrum of the ten semi-artificial motions is quite close to the target design spectrum, a fact that eliminates the differences between design and applied actions as a potential source of any observed undesirable response. Each synthetic motion pair, derived from the two horizontal components of each historical record, was applied twice by mutually changing the components along the x and y system axes. Thus, each design case was analyzed for ten sets of 2-component motions and mean values of peak response indices were computed. In this manner, the effects of individual motions are smoothed and the conclusions become less dependent on specific motion characteristics.

3. Non-linear dynamic analyses

The non linear analyses were carried out using the program RUAUMOKO (Carr 2005). Frame beams and columns were modeled with the well-known plastic hinge model, in which yielding at

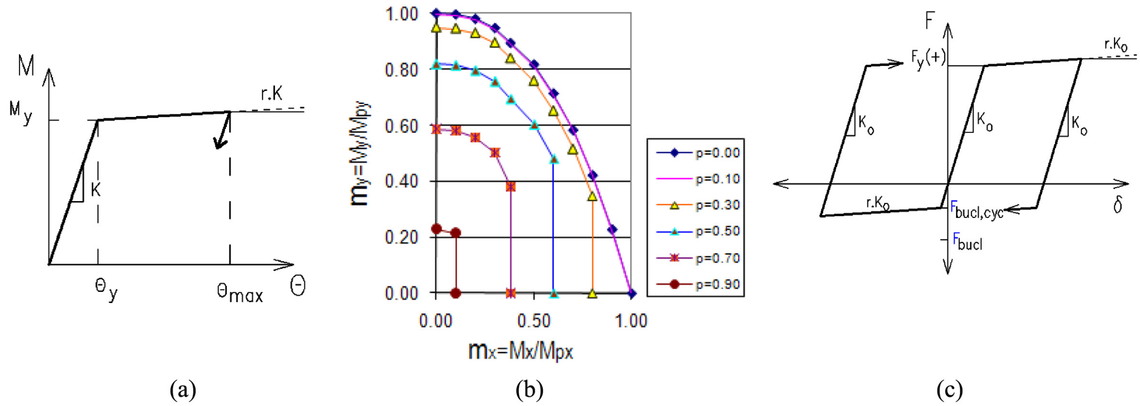

Fig. 3 (a) Nonlinear moment-rotation relations for beam-columns, (b) Column M-N interaction diagram and (c) Nonlinear force deformation diagram for braces member ends is idealized with plastic hinges of finite length having bilinear moment-curvature relationship and strain hardening ratio equal to 0.05 (Fig. 3(a)). A moment-axial force interaction diagram was also employed for columns, giving the yield moment as a function of the applicable axial force on the column section (Fig. 3(b)). Bracing members, yielding in tension and buckling in compression, were modeled with a non-symmetric bilinear force-axial deformation relationship (Fig. 3(c))

The basic measure used to assess the severity of inelastic response is the ductility factor of the various members. For bracing members the ductility factor is defined as

$$\mu_u = 1 + \left(\frac{u_p}{u_y}\right) \tag{3}$$

where u_p is the plastic part of the member elongation and u_y the elongation at first yield.

For beams and beam-columns the rotational ductility factor has traditionally been defined as

$$\mu_\theta = 1 + \left(\frac{\theta_p}{\theta_y}\right) \tag{4}$$

where θ_p is the maximum plastic hinge rotation at either end of a member (beam or column) and θ_y is a normalizing "yield" rotation, typically set equal to $\theta_y = M_y l/6EI$. For columns, the yield moment M_y is usually taken to correspond to the yield moment under the action of gravity loads. In the present study, an alternative definition of the rotational ductility factor, based on the post yield plastic moment, has been used (Anagnostopoulos 1981)

$$\mu = 1 + \left(\frac{\Delta M}{p \cdot M_y}\right) \tag{5}$$

where: $\Delta M = M_{\max} - M_y$, M_y = yield bending moment and $p = 0.05$, the strain hardening ratio.

In addition to the above measures, peak floor displacements and interstory drifts are used to assess the inelastic behaviour of the buildings.

4. Results

The response indices to be presented below for the various buildings are mean values of the peak response parameters over the ten pairs of applied motions. In the case of beam ductility factors, the response parameter averaged over the 10 pairs of motion is the maximum rotational ductility factor in any of the beams in the considered frame and floor. The results are presented for each group of buildings separately.

4.1 One-story frames

Results for the one story frames are summarized in Tables 2 and 3. Ductility factors are listed only for beams and brace members because the columns remained essentially elastic. Looking into Table 2 we see that as expected, displacements at the "flexible" edge of the two eccentric buildings

Table 2 Edge displacements for 1-story frames

	DIRECTION Y		DIRECTION X	
ECCEN-TRICITY	FLEX-EDGE (FR6Y)	STIFF- EDGE (FR1Y)	FLEX-EDGE (FR1X)	STIFF- EDGE (FR4X)
$\varepsilon = 0.00$	**0.02657**	**0.02661**	**0.01454**	**0.01490**
$\varepsilon = 0.10$	**0.03573**	**0.02525**	**0.01908**	**0.01530**
$\varepsilon = 0.20$	**0.03622**	**0.01947**	**0.01976**	**0.01299**

Table 3 Member ductility factors for 1-story frames

	BRACES		BEAMS	
	DIRECTION Y			
ECCEN-TRICITY	FLEX-EDGE (FR6Y)	STIFF-EDGE (FR1Y)	FLEX-EDGE (FR6Y)	STIFF-EDGE (FR1Y)
$\varepsilon = 0.00$	**2.82**	**2.82**	**1.00**	**1.02**
$\varepsilon = 0.10$	**3.80**	**2.67**	**1.08**	**1.00**
$\varepsilon = 0.20$	**3.86**	**2.05**	**1.58**	**1.00**
	DIRECTION X			
ECCEN-TRICITY	FLEX-EDGE (FR1X)	STIFF-EDGE (FR4X)	FLEX-EDGE (FR1X)	STIFF-EDGE (FR4X)
$\varepsilon = 0.00$	**1.50**	**1.56**	**1.00**	**1.03**
$\varepsilon = 0.10$	**1.99**	**1.60**	**1.06**	**1.02**
$\varepsilon = 0.20$	**2.07**	**1.35**	**1.25**	**1.00**

are, as expected, substantially greater than those at the stiff edge due to the induced earthquake rotations (it is for this reason that the edge with the largest displacements has been called "flexible edge" and the opposite edge with the lowest displacement the "stiff edge"). While this was expected, Table 3 indicates that also ductility demands are higher at the flexible edges (along both axes x and y), confirming similar findings for concrete buildings.

4.2 Three-story frames

Displacement results for the 3 story frames are shown in Figs. 4 and 5 for biaxial mass eccentricities ε_m = 0.10 and 0.20. The mean, approximate, floor physical eccentricities, as explained earlier, can be seen in Table 1. Results are as would have been expected: Larger total and interstory displacements at the "flexible" edges than the "stiff" edges in both the "x" and "y" directions as a result of torsion. The corresponding numbers for the torsionally balanced cases are also shown in the various graphs. Moreover, the differences between the two sides increase with the increase in eccentricity (compare Figs. 4 and 5)

Ductility demands in the braces and the beams of the same buildings are shown in Figs. 6 and 7, for ε_m = 0.10 and 0.20, respectively. It is observed that although the ductility factors in all cases are within acceptable levels, the demands for both member types, braces and beams, at the "flexible" edges of the buildings are substantially higher than those of the members at the "stiff" edges, thus making the former more vulnerable. The demands in the torsionally balanced cases are also shown in the various graphs and in almost all cases are somewhere in the middle between the two

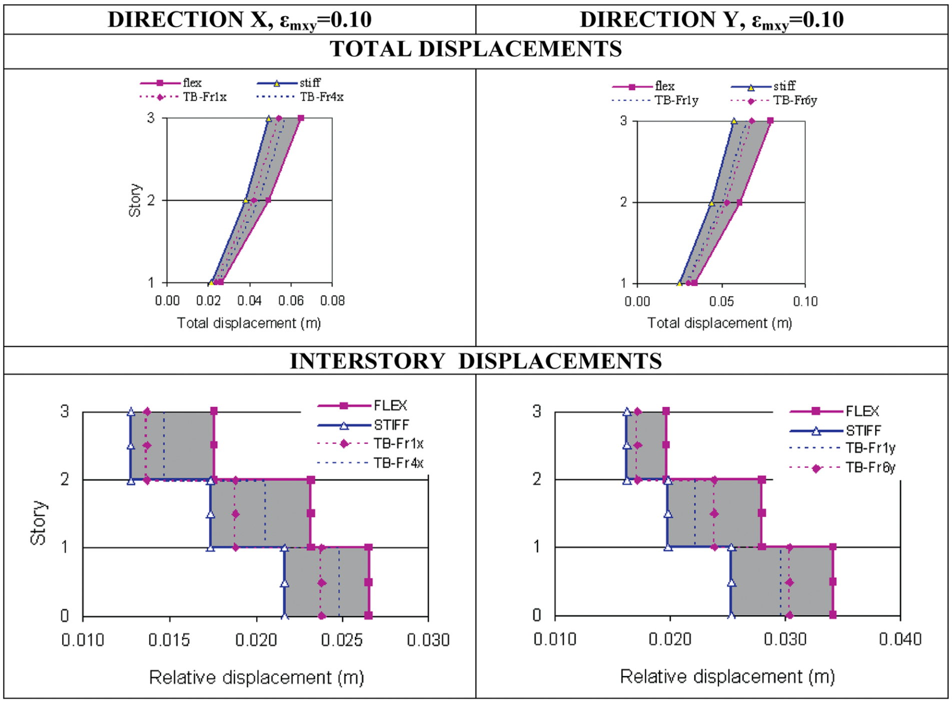

Fig. 4 Total displacements and interstory drifts of 3-story buildings with ε_m = **0.10** and comparison with torsionally balanced (TB) building

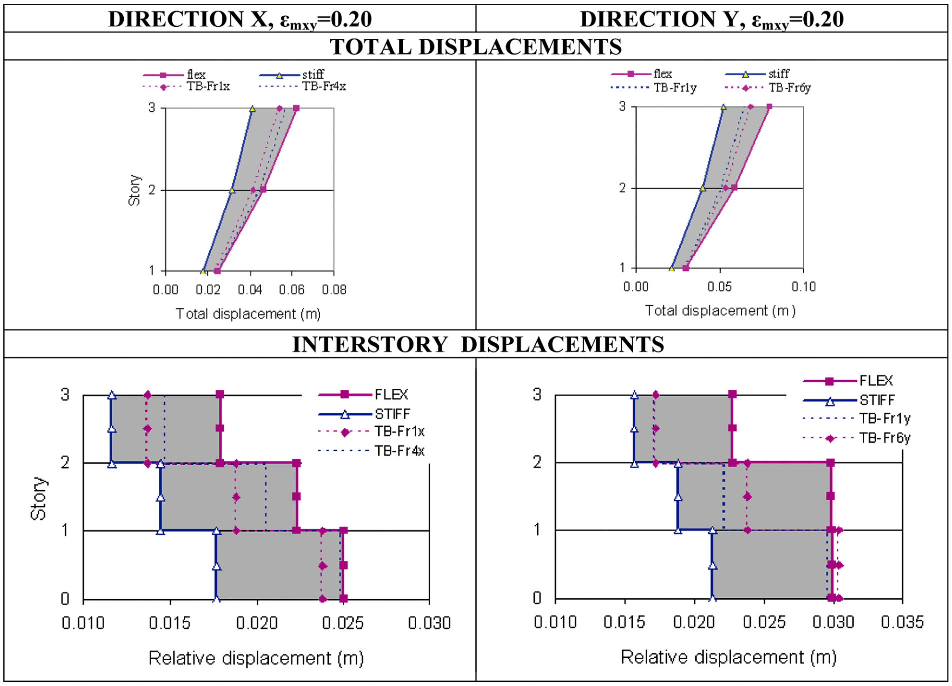

Fig. 5 Total displacements and interstory drifts of 3-story buildings with am ε_m = **0.20** and comparison with torsionally balanced (TB) building

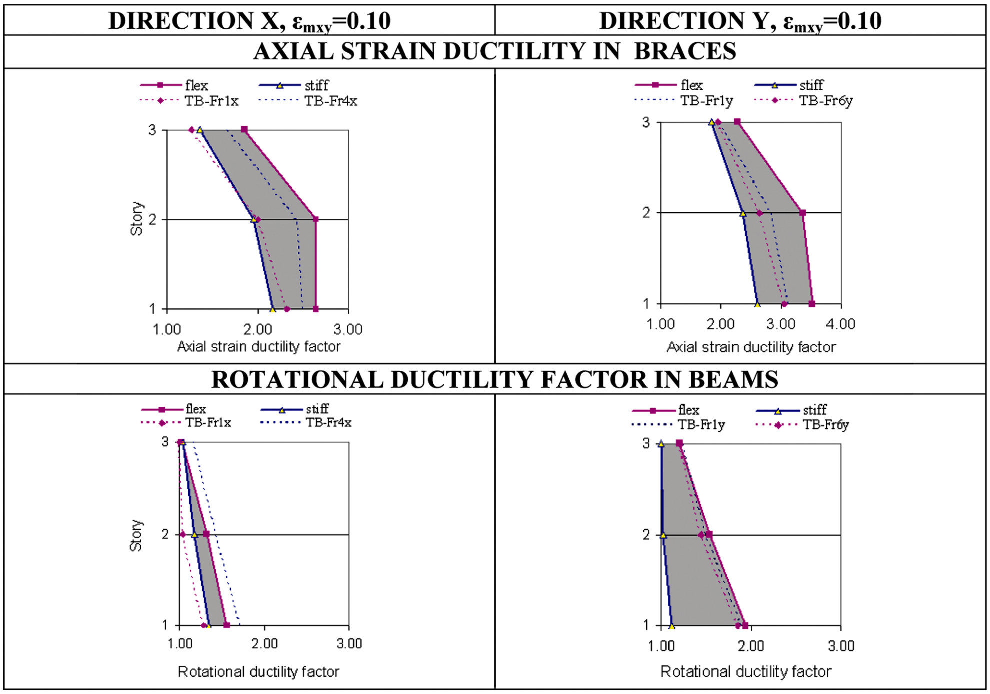

Fig. 6 Member ductility demands of 3-story buildings with am ε_m = **0.10** and comparison with torsionally balanced (TB) building

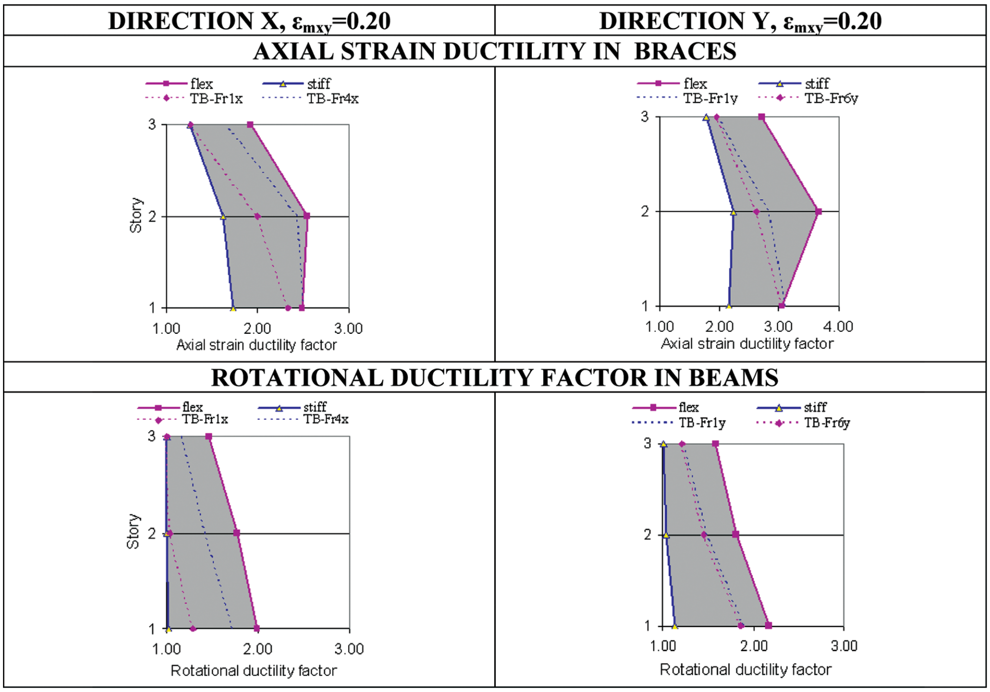

Fig. 7 Member ductility demands of 3-story buildings with am ε_m = **0.20** and comparison with torsionally balanced (TB) building

extremes. Again, the differences between the two edges, “flexible” and “stiff”, increase with increasing eccentricity.

4.3 Five-story frames

The corresponding results, displacements and ductility factors, for the 5 story frame buildings are given in Figs. 8-11. We observe again the same general behavior as for the 3-story buildings.

Although ductility factors are within acceptable limits, the substantial differences between “flexible” and “stiff” edges indicate an undesirable, non uniform distribution of such demands that in case of overload, e.g. under a stronger than anticipated earthquake, may lead to premature failures of members at the “flexible” edges of the non-symmetric building. We also notice here that the differences between “stiff” and “flexible” edge appear greater along the Y direction, a fact that can be explained by the longer sides along the X axis and hence the larger effects of torsion at the Y direction edges. It is rather obvious that a desirable design should aim at minimizing such differences. We note here that the results herein indicate quite clearly that the “critical” elements in non-symmetric buildings are elements at the “flexible” edge , not at the “stiff” edge, as it has been reported in the past and supported by analyses based on oversimplified, one story, 3-degree of freedom systems (Chandler and Duan 1991, Chopra and Goel 1991, Tso and Zhu 1992, Duan and Chandler 1993, Humar and Kumar 1999). This is in agreement with results reported in (Stathopoulos 2001, Stathopoulos and Anagnostopoulos 2002, 2005).

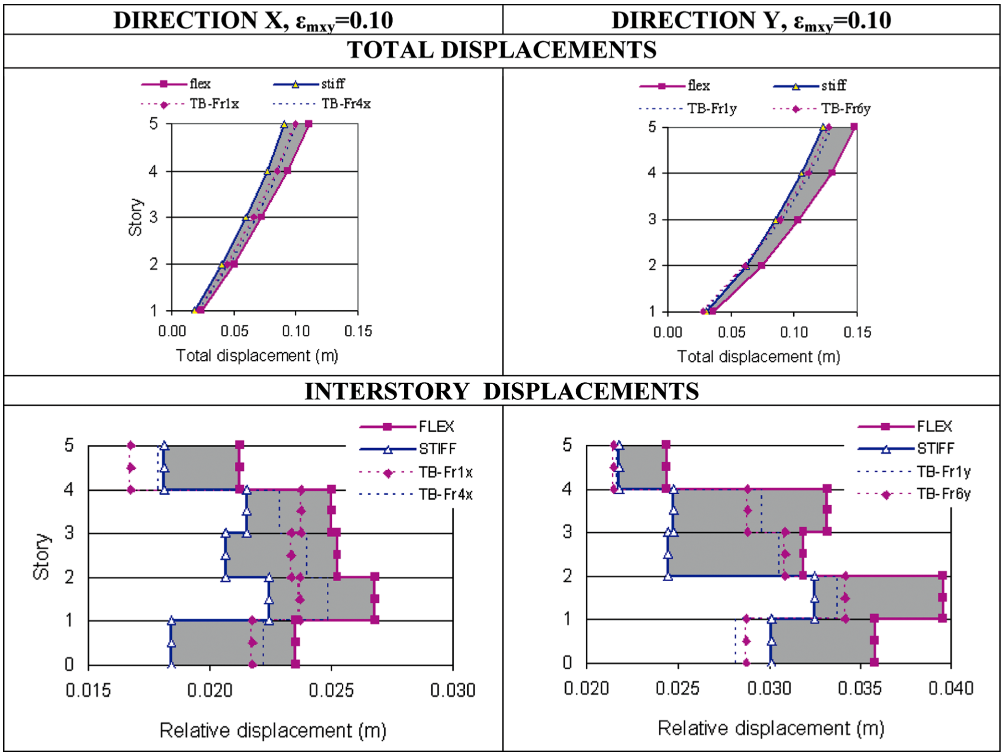

Fig. 8 Total displacements and interstory drifts of 5-story buildings with ε_m = **0.10** and comparison with torsionally balanced (TB) building

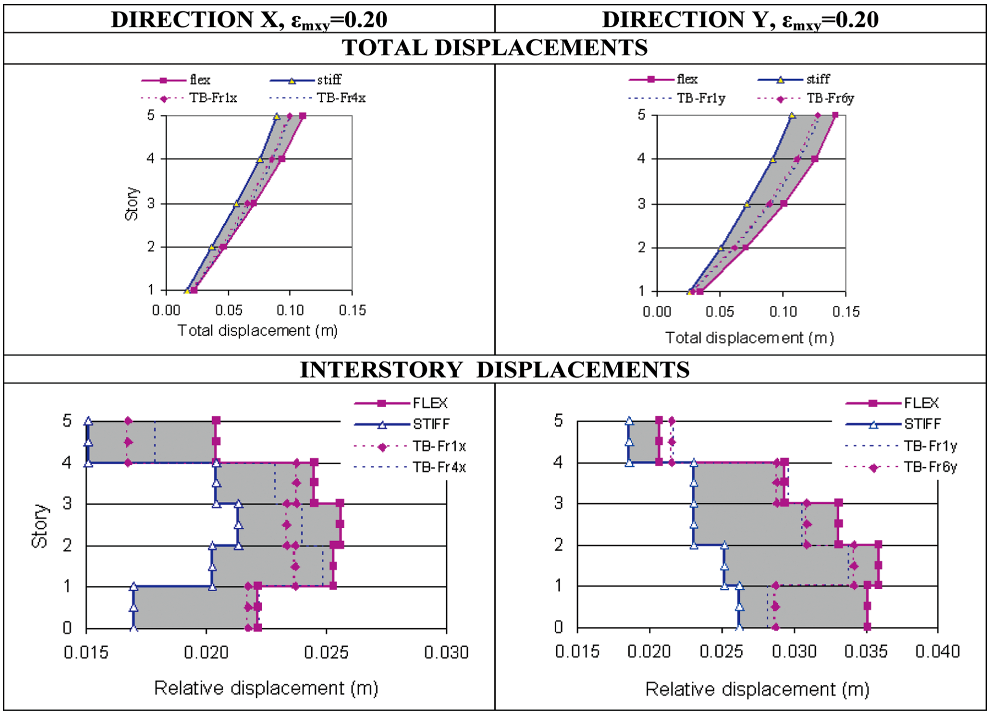

Fig. 9 Total displacements and interstory drifts of 5-story buildings with ε_m = **0.20** and comparison with torsionally balanced (TB) building

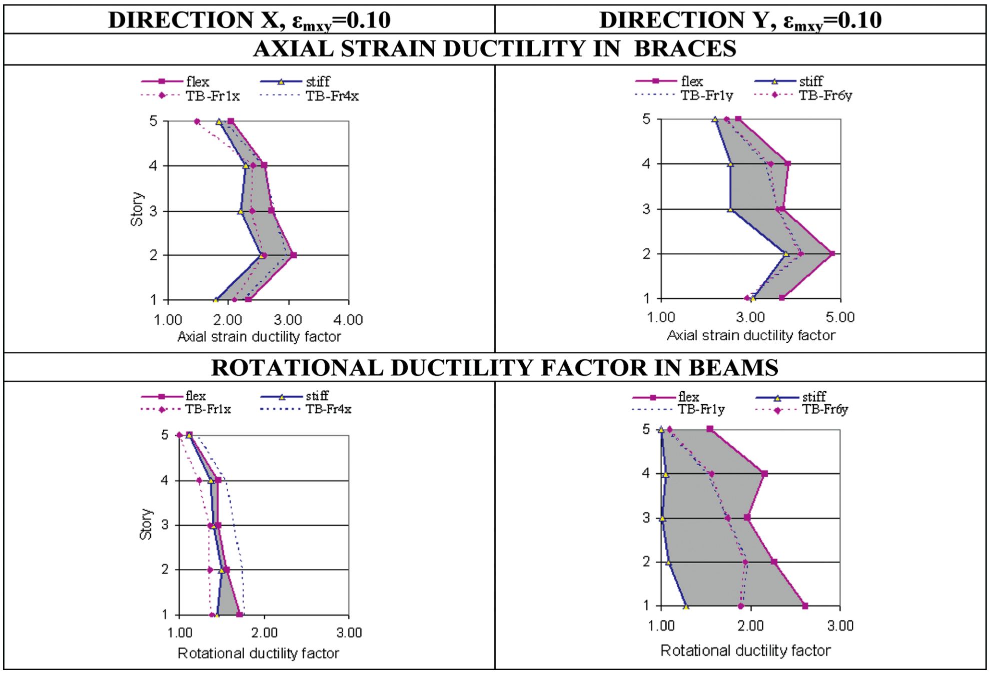

Fig. 10 Member ductility demands of 5-story buildings with ε_m = **0.10** and comparison with torsionally balanced (TB) building

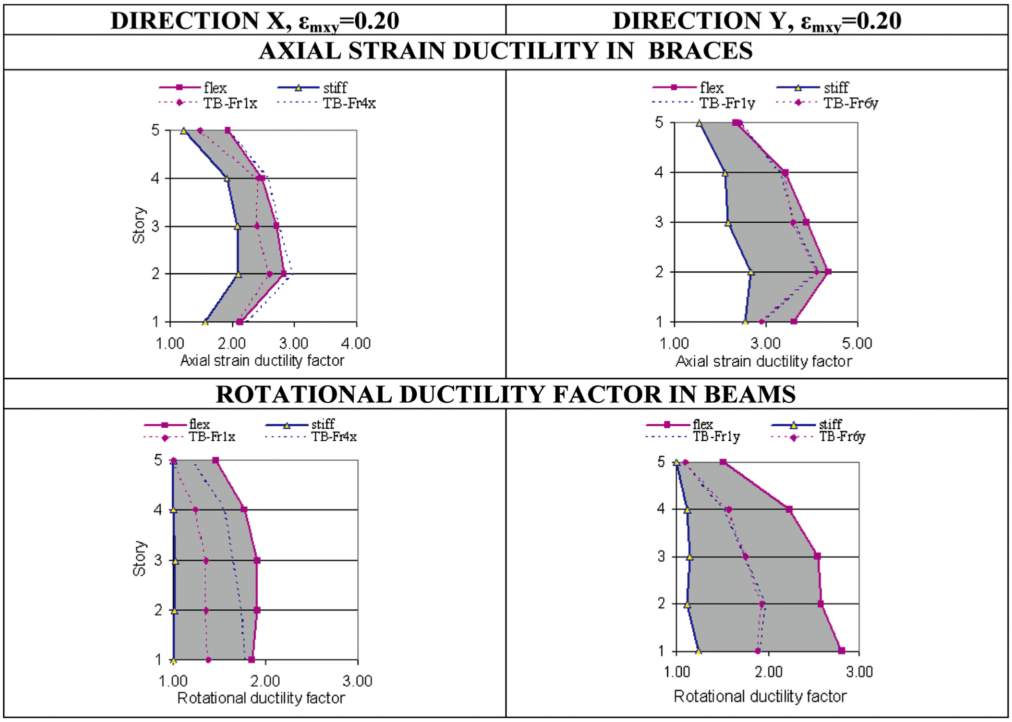

Fig. 11 Member ductility demands of 5-story buildings with ε_m **= 0.20** and comparison with torsionally balanced (TB) building

4.4 Frame stiffness and strengths in a typical eccentric building

In order to get a more clear picture of the stiffness and strength distribution in the load bearing elements, produced by applying the code for a typical design of an eccentric building, pushover analyses were carried out for the plane frames of the 3-story eccentric building having an initial mass eccentricity $\varepsilon_m = 0.20$. These curves are shown in Figs. 12 and 13 for the frames along the y and x axes, respectively. We note that all member properties of this building are listed in the Appendix. We see that along the y axis, the frame at the “flexible” edge, Frame - 6Y, is stiffer and stronger than the frame at the “stiff” edge, Frame - 1Y. This is as expected because for the elastic design the “flexible” edge experiences not only higher earthquake displacements and hence loads, but also higher gravity loads due to the pre selected non-symmetric vertical load distribution that generated the desired initial mass eccentricity of $\varepsilon_m = 0.20$. Along the x axis, the opposite happens: here the “stiff” edge frame, Frame - 4X, is stiffer and stronger than the flexible edge frame, Frame - 1X. This is due to the initial selection of two braced bays in the “stiff” edge and one in the “flexible” edge, in order to have also stiffness eccentricity from the start. We see here that the resisting frame strengths and stiffnesses are as one would have expected from a typical application of the code to the selected building layouts. Yet, the inelastic analyses results indicate that these do not lead to similar (more or less) ductility demands throughout the building layout. It is interesting to also see the overstrength of each of these frames, by looking at the values of the design base shears, marked on each curve and also listed at the bottom of each graph. We note here that these are envelope values that result by applying a total of 32 earthquake loading combinations arising

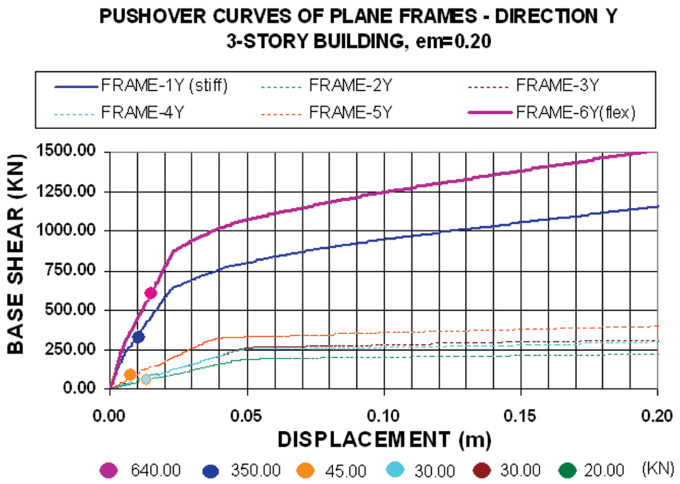

Fig. 12 Comparison of pushover curves. 3-story building, ε_m = **0.20**, direction *Y*. Points on curves with values at bottom indicate the design base shears

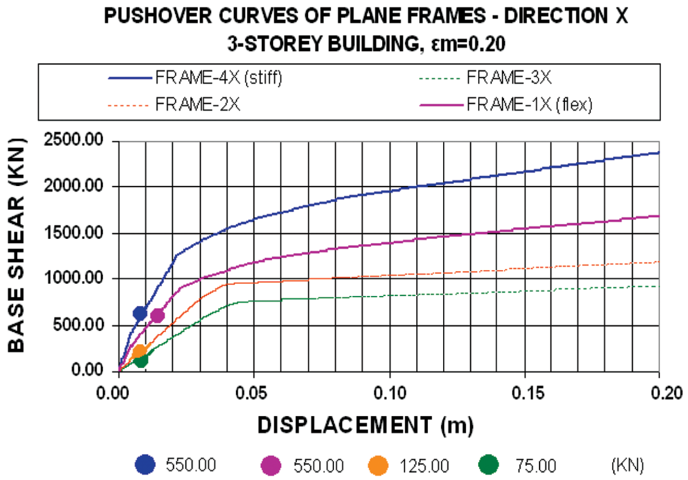

Fig. 13 Comparison of pushover curves. 3-story building, ε_m = **0.20**, direction *X*. Points on curves with values at bottom indicate the design base shears

from 8 loadings ±(Ex + 0.3Ey), ±(Ex – 0.3Ey), ±(0.3Ex + Ey), ±(0.3Ex – Ey) and four possible locations of the mass center due to the accidental design eccentricity, as specified by the code. The differences between design shear from earthquake loading alone and overstrength of a code designed frame, is a reason for which results on inelastic torsion, based on simplified models with element strengths determined only from the earthquake loading, can lead to erroneous conclusions and thus should not be used to assess a code, as has often been done in the past (Anagnostopoulos *et al*. 2010)

4.5 A case of overload

To complete this study, we have carried out analyses with increased levels of earthquake shaking,

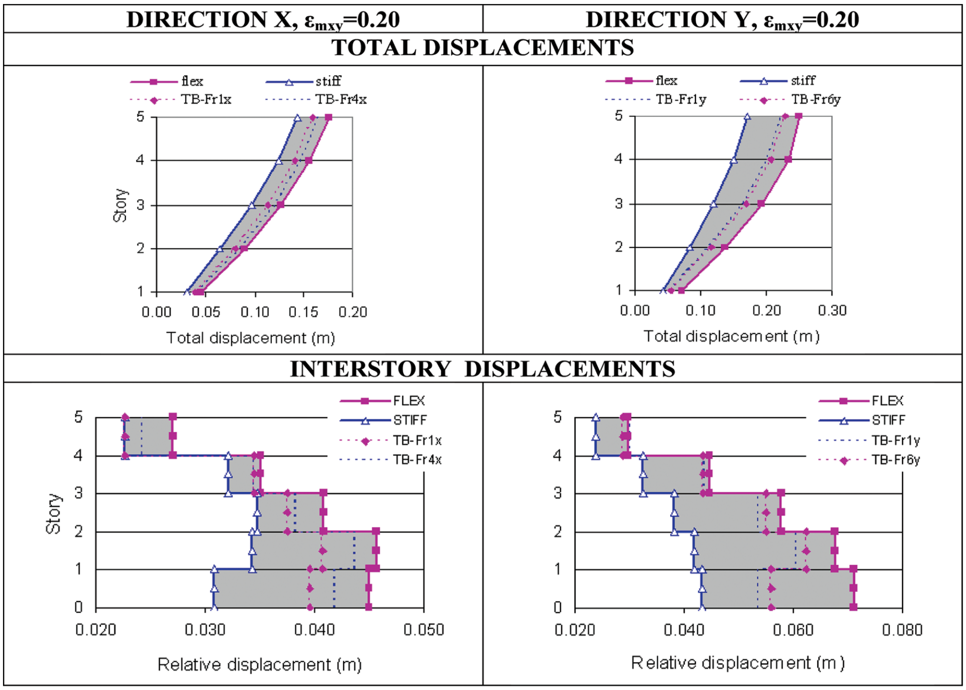

Fig. 14 Total displacements and interstory drifts of 5-story buildings with ε_m = **0.20** for 50% overload and comparison with torsionally balanced (TB) building

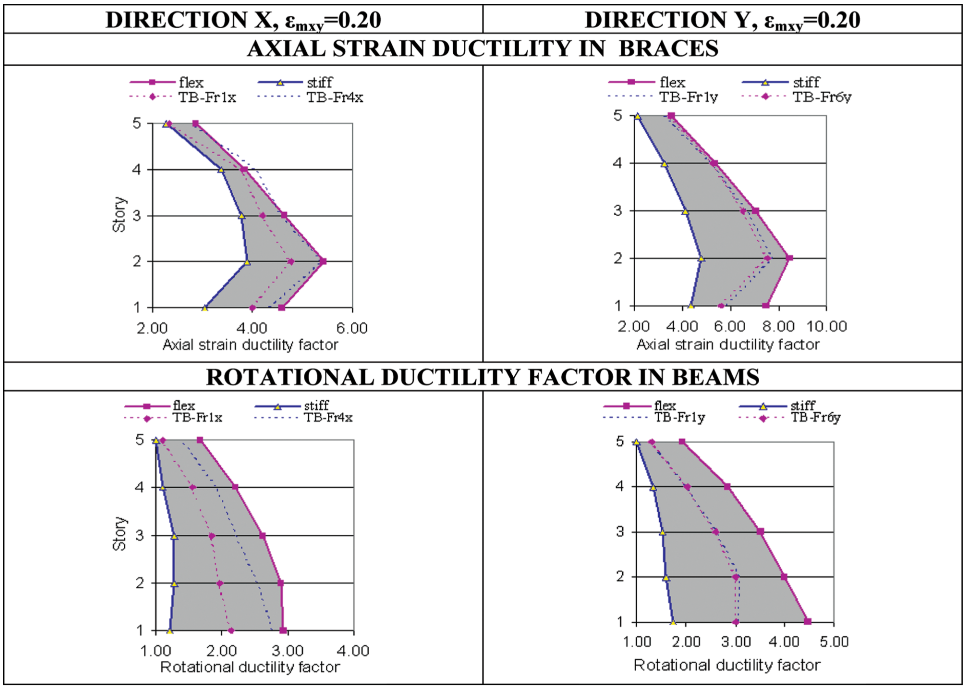

Fig. 15 Member ductility demands of 5-story buildings with ε_m = **0.20** for 50% overload and comparison with torsionally balanced (TB) building

above the design level, in order to see the effects of overloading on members at the two edges, “stiff” and “flexible”. Fig. 14 shows total displacements and interstory drifts and Fig. 15 shows ductility demands for the 5-story eccentric building with $e_m = 0.20$ as well as for the corresponding torsionally balanced building, subjected to the same group of motions scaled up by 50%. All the response parameters indicate the overloading of the flexible edges as compared to the response of the torsionally balanced building and hence the increased risk of failure.

5. Conclusions

Prompted by earlier findings for reinforced concrete frame type buildings, the nonlinear behavior of code designed, non symmetric, braced steel buildings subjected to strong earthquake ground motions was investigated herein. To cover a wide range of building heights and periods, three sets of buildings were designed: with one, three and five stories. In each set, a torsionally balanced building was first designed and subsequently eccentric variants were generated and designed having initial biaxial mass eccentricities of 0.10 and 0.20. The final designs are mass and stiffness eccentric with biaxial physical eccentricities in the range of 0.07 - 0.185. The torsionally balanced building in each group is used for reference. Based on non linear inelastic dynamic analyses of detailed structural models of the plastic hinge type, for 10 sets of two component semi-artificial earthquake motions, it was found for all cases that:

1. The distribution of ductility demands in the non symmetric buildings is far from desirable: Elements at the “flexible” edges of the buildings exhibit much higher ductility demands than elements in the “stiff” edges.
2. This previous result provides a firm and, we dare say, conclusive answer to the widely debated issue in the past, i.e. whether the “stiff” or “flexible” edge elements in non symmetric buildings are the critical elements.
3. Although the ductility demands of all the buildings were within acceptable limits, the substantial differences in ductility demands between “stiff” and “flexible” edges indicate a need for code modification aiming at more uniform distribution of such demands. This would imply avoidance of under (or over) designs and thus a reduced risk of failure in cases of overloads, e.g. when an earthquake stronger than the design earthquake strikes the building.

Acknowledgements

The authors would like to thank Mr. Nikos Chroneas, for making available to them the commercial program NEXT used in the design of all the buildings.

References

Anagnostopoulos, S.A., Alexopoulou, C. and Stathopoulos, K. (2010), “An answer to an important controversy and the need for caution when using simple models to predict inelastic earthquake response of buildings with torsion”, *Earthq. Eng. Struct. Dyn.*, **39**(5), 521-540.

Carr, A.J., (2005), *RUAUMOKO manual: theory and user-guide to associated programs*, Vol.1, Univ. of

Canterbury, New Zealand.
Chandler, A.M and Duan, X.N. (1991), "Evaluation of factors influencing the inelastic seismic performance of torsionally asymmetric buildings", *Earthq. Eng. Struct. Dyn.*, **20**(1), 87-95.
Chopra, A.K. and Goel, R. (1991), "Evaluation of torsional provisions in seismic codes", *J. Struct. Eng.* - ASCE, **117**(12), 3762-3782.
Duan, X.N. and Chandler, A.M. (1993), "Inelastic seismic response of code-designed multistory frame buildings with regular asymmetry", *Earthq. Eng. Struct. Dyn.*, **22**(5), 431-455.
EC3 - Eurocode 3, (2004), "Design provisions for steel structures", *Eur. Prestandard*, CEN 1994; Doc.CEN/TC250/SC8/N (Latest Edition: Eurocode 8: Design of structures for earthquake resistance, European Standard EN1998-1:2004)
EC8 - Eurocode 8, (2004), "Design provisions for earthquake resistance of structures", *Eur. Prestandard*, CEN 1994; Doc.CEN/TC250/SC8/N (Latest Edition: Eurocode 8: Design of structures for earthquake resistance, European Standard EN1998-1:2004).
EAK2000 (2000), "Greek code for earthquake resistant design", *Greek Ministry of Environment, City Planning and Public Works* 2000.
Humar, J.L. and Kumar, P. (1999), "Effect of orthogonal in plane structural elements on inelastic torsional response", *Earthq. Eng. Struct. Dyn.*, **28**(10), 1071-1097.
Karabalis, D.L., Cokkinides, G.J., Rizos, D.C., Mulliken, J.S. and Chen, R. (1994), "An interactive computer code for generation of artificial earthquake records", *Computing in Civil Engineering (ASEE)* 1994, K. Khozeimeh (ed.) 1122-1155.
Kyrkos, M. and Anagnostopoulos, A. (2010), "Towards earthquake resistant design of steel buildings for uniform ductility demands", *Invited paper, Proc., SEMC 2010: The Fourth International Conference on Structural Engineering, Mechanics and Computation : 135-140*, Cape Town, South Africa, A. Zingoni (ed.), CRC Press Balkema 2010.
Rutenberg, A. (2002), "Behavior of irregular and complex structures - Progress since 1998", EAEE Task Group (TG)8, *Proc 12th European Conference on Earthquake Engineering*, London, Elsevier No.832.
Stathopoulos, K.G. (2001), "Investigation of the inelastic response and earthquake resistant design of asymmetric buildings", *Ph.D. Dissertation*, University of Patras, Greece. (in Greek)
Stathopoulos, K.G. and Anagnostopoulos, S.A. (2002), "Inelastic earthquake induced torsion in buildings: results from realistic models", Proceedings, *12th European Conference on Earthquake Engineering,* Paper no.453, London, UK.
Stathopoulos, K.G. and Anagnostopoulos, S.A. (2005) "Inelastic torsion of multistory buildings under earthquake excitations", *Earthq. Eng. Struct. Dyn.*, **34**(12), 1449-1465.
Tso, W.K. and Zhu, T.J. (1992), "Design of torsionally unbalanced structural systems based on code provisions I: Ductility demand", *Earthq. Eng. Struct. Dyn.*, **21**(7), 609-627.

CC

Appendix

List of member sections of 3-story eccentric building with $\varepsilon_m = 0.20$

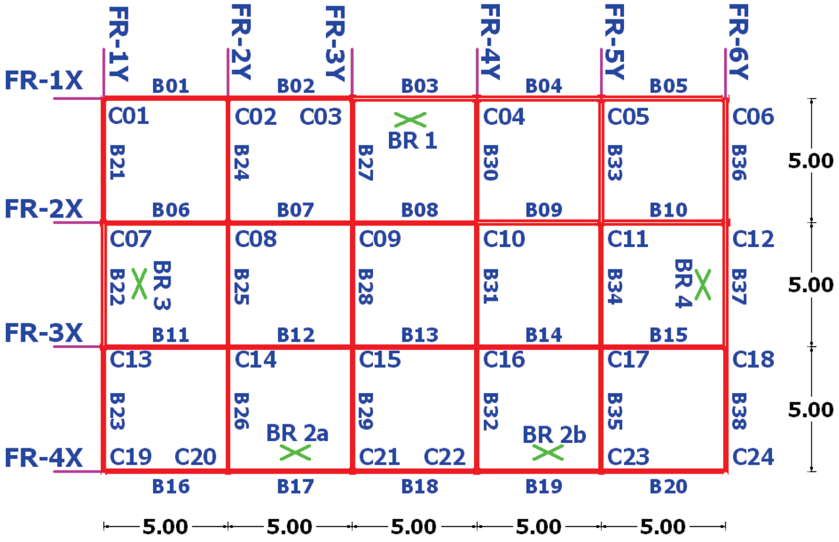

Member Location

COLUMN SECTIONS

COLUMNS	1st story	2nd story	3rd story		COLUMNS	1st story	2nd story	3rd story
C01	HEB 160	HEB 160	HEB 160		**C13**	HEB 260	HEB 240	HEB 220
C02	HEB 180w	HEB 180w	HEB 180w		**C14**	HEB 220	HEB 200	HEB 200
C03	HEB 240w	HEB 200w	HEB 160w		**C15**	HEB 220	HEB 200	HEB 200
C04	HEB 220w	HEB 200w	HEB 180w		**C16**	HEB 240	HEB 220	HEB 220
C05	HEB 280w	HEB 260w	HEB 260w		**C17**	HEB 240	HEB 220	HEB 200
C06	HEB 240	HEB 240	HEB 240		**C18**	HEB 320	HEB 300	HEB 260
C07	HEB 260	HEB 220	HEB 220		**C19**	HEB 200	HEB 180	HEB 180
C08	HEB 240	HEB 220	HEB 220		**C20**	HEB 220w	HEB 200w	HEB 200w
C09	HEB 240	HEB 220	HEB 220		**C21**	HEB 220w	HEB 200w	HEB 200w
C10	HEB 240	HEB 220	HEB 220		**C22**	HEB 220w	HEB 200w	HEB 200w
C11	HEB 300	HEB 300	HEB 280		**C23**	HEB 220w	HEB 200w	HEB 200w
C12	HEB 360	HEB 340	HEB 280		**C24**	HEB 240	HEB 240	HEB 220

w: denotes that the weak axis of the steel profile is parallel to the *Y*-axis

BEAM SECTIONS

B01	IPE 160	**B10**	IPE 450	**B19**	IPE 140	**B29**	IPE 200
B02	IPE 140	**B11**	IPE 200	**B20**	IPE 140	**B30**	IPE 240
B03	IPE 140	**B12**	IPE 200	**B21**	IPE 160	**B31**	IPE 200
B04	IPE 160	**B13**	IPE 200	**B22**	IPE 140	**B32**	IPE 200
B05	IPE 220	**B14**	IPE 200	**B23**	IPE 140	**B33**	IPE 360
B06	IPE 220	**B15**	IPE 330	**B24**	IPE 240	**B34**	IPE 300
B07	IPE 220	**B16**	IPE 140	**B25**	IPE 200	**B35**	IPE 220
B08	IPE 200	**B17**	IPE 140	**B26**	IPE 200	**B36**	IPE 240
B09	IPE 220	**B18**	IPE 140	**B27**	IPE 240	**B37**	IPE 220
				B28	IPE 200	**B38**	IPE 140

BRACES (Circular Cross Sections)

	1st story	**2nd story**	**3rd story**
FR-1X	193.7×6	139.7×6	88.9×5
FR-4X	168.3×5	139.7×5	88.9×4
FR-1Y	168.3×5	139.7×5	88.9×4
FR-6Y	193.7×6	139.7×6	88.9×5